Techno-Economic Screening of Surfactant Flooding in High-Temperature, High-Salinity Carbonates under Retention Uncertainty

Imad A. Adel[a], Alvaro Moralez[a], Emad W. Al-Shalabi[a,b],Waleed Alameri[a,b]
[a] *Chemical and Petroleum Engineering Department, Khalifa University of Science and Technology, Abu Dhabi, United Arab Emirates*
[b] *Research and Innovation Center on CO_2 and Hydrogen, Khalifa University of Science and Technology, Abu Dhabi, UAE*
[c] *Abu Dhabi National Oil Company (ADNOC), Abu Dhabi, United Arab Emirates*

** Manuscript under review at **Petroleum Research** (KeAi Publishing).*

Abstract

Mature high-temperature, high-salinity (HTHS) carbonate assets may contain residual oil that is technically accessible but economically sensitive to chemical efficiency. This study develops a scenario-based techno-economic screen for surfactant flooding in HTHS carbonates, using dynamic surfactant retention (Γ) as the central bridge variable linking laboratory performance to economic value. A screened benchmark of 12 optimized Guerbet alkoxy carboxylate/internal olefin sulfonate corefloods relates retention to laboratory tertiary recovery within the calibrated range Γ = 0.083–0.33 mg/g-rock, yielding the empirical fit $RF_{lab} = 108 \times \exp(-1.23\Gamma)$ with R^2 = 0.90 and RMSE = 3.0% S_{orw}. Contextual field cases from Kuwait, the UAE, and Oman provide operability evidence but are not used to calibrate the model.

The benchmark is coupled to a deterministic discounted-cash-flow (DCF) screen for a representative brownfield carbonate sector. At the base case (Γ = 0.20 mg/g-rock, Brent = 60 USD/bbl), the model yields NPV_{10} = 7.2 MMUSD, IRR = 20.7%, UTC = 55.0 USD/bbl, and incremental oil recovery of 3.48 MMstb. Screening breakeven occurs at Γ = 0.24 mg/g-rock (60 USD/bbl) and Brent = 57.3 USD/bbl (Γ = 0.20 mg/g-rock). Sensitivity ranking identifies retention, saturation state, and volumetric sweep efficiency as the dominant value drivers, with operational cost parameters forming a middle tier and macro-financial inputs the lowest. The framework supports candidate ranking and pilot screening rather than field prediction.

Keywords: techno-economic screening, surfactant flooding, carbonate reservoirs, retention uncertainty, brownfield recovery, HTHS.

1. Introduction

Mature carbonate assets may retain substantial post-waterflood oil, but incremental recovery in high-temperature, high-salinity (HTHS) settings is a brownfield capital-allocation problem rather than a chemistry problem alone (Sheng, 2011; Mogensen and Masalmeh, 2020; Henthorne et al., 2014). Candidate chemical EOR projects compete for investment under uncertainty in contacted volume, chemical efficiency, production timing, and unit cost (Henthorne et al., 2014; Jabbar et al., 2017; Al-Murayri et al., 2022). A useful screening framework, therefore, needs to connect technically measurable variables to bounded economic outputs under clearly stated assumptions.

HTHS carbonate conditions are among the most restrictive environments for surfactant flooding. Reservoir temperatures commonly exceed 75–80 °C, and formation-brine salinities can exceed 80,000 ppm TDS (Sheng, 2011; Mogensen and Masalmeh, 2020). Carbonate heterogeneity, microporosity, and permeability contrast limit contacted volume, while temperature, divalent ions, and salinity narrow the formulation window (Hirasaki and Zhang, 2004; Adkins et al., 2012; Sheng, 2011; Lu et al., 2014; Mogensen and Masalmeh, 2020). Throughout this paper, formation-brine salinity is distinguished from injected-slug salinity because optimum-salinity designs often use softened injection brines substantially below native formation-brine salinity.

Over the last fifteen years, large-hydrophobe surfactant systems based on Guerbet alkoxy carboxylates (GAC) and internal olefin sulfonates (IOS) have improved technical operability in selected HTHS carbonate systems (Solairaj et al., 2012; Lu et al., 2014; Upamali et al., 2018). Published laboratory studies report Type III microemulsion behavior, low interfacial tension, wettability alteration, and dynamic retention substantially below the levels reported for earlier carbonate formulations (Solairaj et al., 2012; Lu et al., 2014; Al-Murayri et al., 2017; Upamali et al., 2018; Abalkhail et al., 2020). Field and one-spot programs from Kuwait, the UAE, and Oman indicate that implementation remains sensitive to injectivity, sweep, conformance, salinity control, and formulation stability (Al-Amrie et al., 2015; Morel et al., 2016; Al-Murayri et al., 2022; Wang et al., 2024; Karpan et al., 2025).

Despite these advances, the link between laboratory retention measurements and economically relevant field screening remains weakly standardized for HTHS carbonates (Solairaj et al., 2012; Jabbar et al., 2017; Abalkhail et al., 2020). Much of the published

literature reports formulation performance in terms of phase behavior, interfacial tension, or tertiary recovery, but fewer studies report dynamic retention in a form that can be transferred into an economic screen (Lu et al., 2014; Jabbar et al., 2017; Upamali et al., 2018; Abalkhail et al., 2020). This study compiles a screened HTHS carbonate benchmark and uses that benchmark to construct a scenario-based techno-economic screening framework in which dynamic surfactant retention is the central uncertainty. Unlike prior techno-economic frameworks that couple laboratory recovery to DCF models using tertiary recovery alone as the bridge variable, this work uses dynamic surfactant retention measured from coreflood material balance, a quantity directly tied to chemical spend and bank propagation, as the explicit link between formulation screening and economic viability. The objective is not field prediction. It is to evaluate how retention, sweep, saturation state, and cost assumptions affect candidate ranking within the calibrated laboratory range and the stated discounted-cash-flow assumptions.

2. Technical Basis for Retention-Sensitive Screening in HTHS Carbonates

2.1. HTHS Carbonate Constraints

Mature HTHS carbonates combine elevated temperature, high salinity, and strong petrophysical heterogeneity. Microporous domains and permeability contrast can contain substantial oil yet contribute little to flow, so laboratory displacement efficiency does not transfer directly to field recovery (Hirasaki and Zhang, 2004; Sheng, 2011; Mogensen and Masalmeh, 2020; Mejía et al., 2021).

Many earlier surfactant systems were unsuitable under carbonate HTHS conditions because thermal degradation, precipitation in the presence of calcium and magnesium ions, chromatographic separation, and adsorption increased chemical loss (Adkins et al., 2012; Lu et al., 2014; Montes et al., 2018; ShamsiJazeyi et al., 2014). For screening purposes, the practical consequence is that value depends on both local displacement efficiency and the fraction of active surfactant that remains mobile within the contacted rock volume.

2.2. Retention Relevance and Screening Variable Definition

In this study, dynamic surfactant retention (Γ) is expressed as milligrams of active surfactant per gram of rock (mg/g-rock) from coreflood material balance unless stated otherwise (Solairaj et al., 2012; Abalkhail et al., 2020). Reported values, therefore, refer primarily to dynamic coreflood mass-balance measurements rather than to static adsorption tests.

In HTHS carbonates, Γ integrates several loss mechanisms, including adsorption, precipitation, phase trapping, and inaccessible-pore losses (Solairaj et al., 2012; ShamsiJazeyi et al., 2014; Abalkhail et al., 2020; Tackie-Otoo et al., 2024). It is therefore used here as the most defensible bridge variable between laboratory performance and the scenario-based economic screen developed in Section 4. As noted in broader chemical EOR reviews, excessive surfactant retention onto rock surfaces can cause considerable financial loss, reinforcing the use of dynamic retention as the central economic screening variable (Lim et al., 2023).

2.3. Displacement Basis and Screening Criteria

The displacement basis retained for screening is conventional. Low interfacial tension and favorable phase behavior mobilize trapped oil, while wettability modification can improve local displacement in mixed-wet carbonate pore systems (Hirasaki and Zhang, 2004; Lu et al., 2014; Mejía et al., 2021; Zahedi and Saeedi Dehaghani, 2025). These mechanisms are included here only to justify the technical basis of the screened benchmark, not to imply field readiness.

Surfactant flooding seeks to reduce oil-water interfacial tension (σ) and increase the capillary number (N_c) sufficiently to mobilize residual oil. Recent HTHS carbonate studies report low interfacial tension together with measurable incremental recovery under 90–120 °C test conditions (Lu et al., 2014; Upamali et al., 2018; Zhou et al., 2021a).

Fig. 1 is retained as a mechanistic anchor for the capillary-desaturation discussion. For mixed- to oil-wet carbonates, the critical N_c required for desaturation is generally higher than in reference water-wet sandstones, so capillary-number escalation and phase-behavior control remain screening-relevant criteria rather than direct field-design rules (Flaaten et al., 2009; Masalmeh, 2013; Humphry et al., 2014).

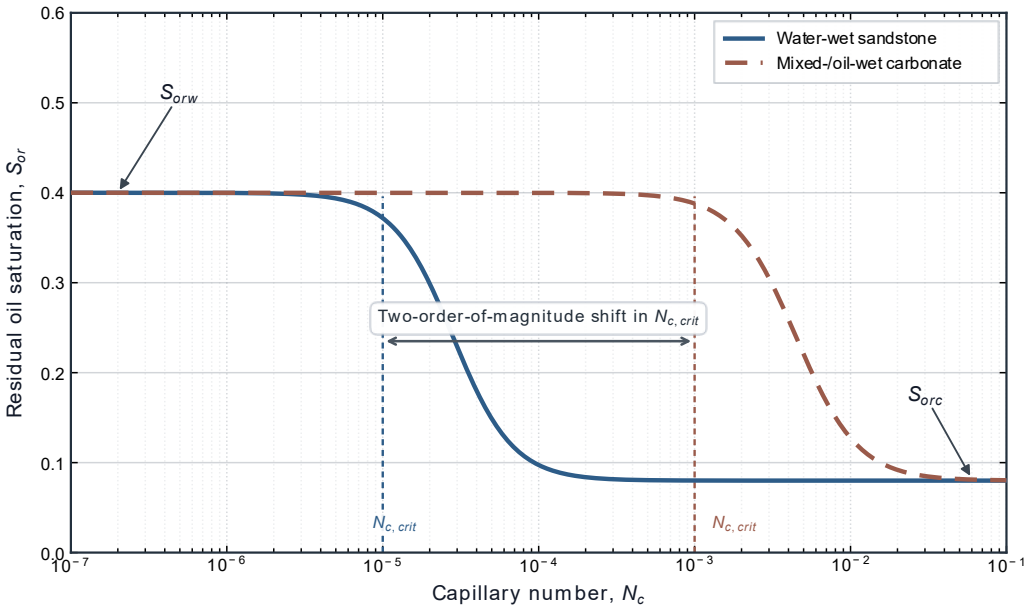

Fig. 1. Capillary desaturation curves showing residual oil saturation (S_{or}) as a function of capillary number (N_c) for carbonate and sandstone matrices.

2.4. Formulation Basis for Benchmark Inclusion

Large-hydrophobe GAC/IOS systems dominate the screened benchmark because they provide a workable balance between brine compatibility, interfacial activity, and adsorption control under severe HTHS carbonate conditions (Lu et al., 2014; Weerasooriya and Pope, 2014; Zhou et al., 2021b). The benchmark was not assembled around molecular novelty alone; it was assembled around technically consistent candidate systems that survived laboratory screening.

Accordingly, the retained studies report HTHS-compatible formulations together with evidence of favorable phase behavior and dynamic retention in a form suitable for screening transfer (Lu et al., 2014; Jabbar et al., 2017; Al-Murayri et al., 2017; Maubert et al., 2018; Upamali et al., 2018; Ghosh and Mohanty, 2019; Abalkhail et al., 2020).

2.5. GAC/IOS Structure–Property Context

GAC surfactants are based on large branched hydrophobes coupled to alkoxy-carboxylate headgroups that are tunable through hydrophobe length and EO/PO block design (Adkins et al., 2012; Lu et al., 2014; Weerasooriya and Pope, 2014; Zhou et al., 2021b). This structure-property flexibility is the main reason they appear repeatedly in HTHS carbonate formulation studies.

The principal design levers are hydrophobe size and the EO/PO balance, which shift optimum salinity, aqueous stability, and adsorption behavior under HTHS conditions; schematic GAC and IOS structures together with a compact structure–property map are therefore moved to Supplementary Figs. S1–S3 as formulation context rather than field-design rules (Levitt et al., 2009; Adkins et al., 2012; Lu et al., 2014; Weerasooriya and Pope, 2014; Zhou et al., 2021b).

Related GAC/IOS laboratory studies also show favorable microemulsion viscosity and low-retention behavior in optimized systems, although some of that evidence comes from sandstone rather than carbonate media (Upamali et al., 2018).

IOS co-surfactants remain relevant because they broaden the low-interfacial-tension window and improve brine tolerance when paired with GAC systems (Lu et al., 2014; Upamali et al., 2018; Zhou et al., 2021b).

Regional carbonate programs have reported large salinity-scan datasets and repeated pipette testing under live-oil and seawater-grade conditions, which support the use of GAC/IOS formulation families as the technical basis of the benchmark subset (Levitt et al., 2016; Jabbar et al., 2017; Montes et al., 2018).

2.6. Why Retention Becomes the Screening Control Variable

Within the screened benchmark and closely related laboratory studies, dynamic retention spans 0.083–0.33 mg/g-rock for the cases retained here (Lu et al., 2014; Al-Murayri et al., 2017; Abalkhail et al., 2020; Panthi and Mohanty, 2024). Across that range,

higher Γ is associated with lower laboratory tertiary recovery, which makes retention the natural control variable for economic screening.

Manufacturing basis, injectivity, produced-fluid handling, and chemical logistics remain relevant contextual constraints for HTHS carbonate projects, but they are not modeled here as independent threshold variables (Morel et al., 2016; Jabbar et al., 2017; Al-Murayri et al., 2018; Al-Murayri et al., 2022). Their role in this manuscript is to explain why formulation stability, compatibility, and implementation practicality must be screened before the techno-economic framework in Section 4 is applied.

2.7. Research Gaps Motivating the Screening Approach

The construction of the HTHS benchmark revealed three methodological gaps in the broader EOR literature:

1. Inconsistency in Retention Reporting: Only a fraction of published studies report retention metrics in a format compatible with economic modeling. Many carbonate coreflood studies report tertiary recovery and IFT but omit adsorption entirely or report only static adsorption on crushed rock. Static measurements do not capture dynamic transport effects such as accessible pore volume and flow-rate dependence. Table 1 addresses this gap by filtering for studies that report dynamic retention (mg/g-rock) derived from material balance.

2. The High-Temperature Data Distribution: The current optimized dataset is clustered in the 78–100 °C window. Data for applications exceeding 110 °C remain sparse, yet several Middle East carbonate reservoirs remain above 110 °C, where hydrolysis kinetics and polymer thermal degradation may shorten effective chemical lifetime. The public domain still lacks a sufficient set of GAC/IOS corefloods under these conditions.

3. Decoupling of Surfactant and Polymer Performance: A final gap lies in the lack of integration between surfactant retention and polymer rheology. In the screening framework, RF_{field} scales with E_v x (S_{orw}/S_{oi}), so mobility control affects NPV through E_v. A moderate-IFT design with higher E_v yields higher NPV than an ultra-low-IFT design with poor sweep when sweep limits incremental recovery. Few studies simultaneously report full viscosity profiles, thermal stability, and surfactant retention for the same core. Comparative polymer-flooding studies have shown that macroscopic sweep efficiency is the dominant factor during recovery and that project success depends on cost analysis of the selected system (Hazarika et al., 2023), yet this kind of integrated technical–economic assessment remains rare for surfactant–polymer systems in HTHS carbonates.

3. Screened Benchmark and Contextual Operability Evidence

3.1. Screened Benchmark Dataset and Inclusion Criteria

To quantify the technical boundaries of the screened benchmark, a dataset of 12 optimized HTHS carbonate corefloods was compiled. Table 1 summarizes the laboratory benchmark subset used for the retention–recovery screening analysis.

To maintain compatibility with the subsequent economic model, the benchmark was restricted to optimized candidate systems that satisfied the reported laboratory screening sequence, including brine compatibility, acceptable phase behavior, and dynamic retention reporting from material balance. Studies that did not report retention on a comparable basis, did not reach the targeted phase-behavior window, or exhibited clear instability were excluded from the quantitative benchmark. The resulting dataset should therefore be read as an upper-bound screened subset rather than as a representative carbonate chemical EOR (CEOR) distribution.

For reproducibility, the benchmark retained studies that reported dynamic retention via material balance at temperature ≥ 78 °C and salinity ≥ 40,000 ppm TDS, with dynamic retention < 0.35 mg/g-rock and tertiary recovery > 50% S_{orw}. These cutoffs define the screened dataset rather than universal performance thresholds.

The retained subset should therefore be interpreted as an upper-bound performance sample of optimized candidate systems rather than as a representative distribution of carbonate CEOR outcomes. Inclusion in Table 1 indicates that the formulation survived laboratory screening; it does not imply field validation or broad portability across HTHS carbonate settings.

When S_{orw} recovery was not explicitly reported, it was calculated from the reported incremental original oil in place (OOIP) recovery using Eq. (1).

$$RF_{lab}\ (\%\ S_{orw}) = (RF_{OOIP} \times S_{oi}) / S_{orw} \quad (1)$$

The calibrated benchmark used in Section 3.2 contains n = 12 coreflood observations over Γ = 0.083–0.33 mg/g-rock. This range and sample size bound the empirical correlation developed below.

Table 1. Screened upper-bound HTHS carbonate coreflood benchmark of optimized GAC/IOS candidate systems used to calibrate the empirical retention-recovery relation

References	Core type	Temp (°C)	Salinity (ppm) (core/slug)	Surfactant family	Additives	Recovery of S_{orw} (%)	Γ (mg/g-rock)
(Lu et al., 2014)	Silurian Dolomite	78	235,400 / 62,700	GAC + IOS	TEGBE, FP 3330S	91.6	0.16
	Reservoir Carbonate	100	66,800 / 38,000	GAC + IOS	FP 3330S	70.3	0.33
(Al-Murayri et al., 2017)	Reservoir Carbonate	78	110,000 / 67,500	GAC + IOS	Phenol-5EO, Hybrid Alkali	76.5	0.26
	Reservoir Carbonate	78	49,964 / 89,964	GAC + IOS	Phenol-4EO, Hybrid Alkali	90.5	0.17
(Jabbar et al., 2017)	Reservoir Carbonate	100	42,800 / 66,000	GAC + IOS	IBA-3EO, NaOH, SAV55	82.0	0.24
(Maubert et al., 2018)	Indiana Limestone	83	75,000 / 58,000	GAC + IOS	IBA-3EO, NaOH, FP 3330S	97.7	0.125
	Indiana Limestone	83	75,000 / 58,000	GAC + IOS	IBA-3EO, NaOH, FP 3330S	85.9	0.174
(Ghosh and Mohanty, 2019)	Indiana Limestone	80	92,336 / 86,000	GAC + IOS	AN-125 VHM	71.0	0.32
	Indiana Limestone	80	92,336 / 79,000	GAC + IOS	Phenol-5EO, AN-125 VHM	81.0	0.20
(Abalkhail et al., 2020)	Indiana Limestone	100	57,539 / 60,000	GAC + IOS	DIPA-10EO, FP 3330S	91.8	0.11
	Reservoir Carbonate	100	57,539 / 60,000	GAC + IOS	DIPA-10EO, NH_4OH	93.6	0.083
(Adel et al., 2025)	Reservoir Carbonate	100	243,000 / 43,373	GAC + IOS	Ethoxylated Phenol	86.4	0.17

Note: *In the additives column, entries are grouped by functional role as reported in the original sources. Polymers: FP 3330S, SAV55, and AN-125 VHM. Co-solvents or nonionic additives: TEGBE, Phenol-4EO, Phenol-5EO, IBA-3EO, and Ethoxylated Phenol. Hybrid alkali/co-solvent additive: DIPA-10EO. Alkalis: Hybrid Alkali, NaOH, NH_4OH. Proprietary or trade names are retained as reported in the cited studies.*

3.2. Empirical Retention–Recovery Relation

Fig. 2 plots the screened benchmark and shows an inverse association between dynamic surfactant retention (Γ) and laboratory tertiary recovery, RF_{lab}, for the optimized candidate systems retained in Table 1. This trend is consistent with surfactant-bank depletion logic reported in the EOR literature (Lake et al., 2014). Over the calibrated range of the screened dataset, the laboratory benchmark is described by the following empirical exponential correlation.

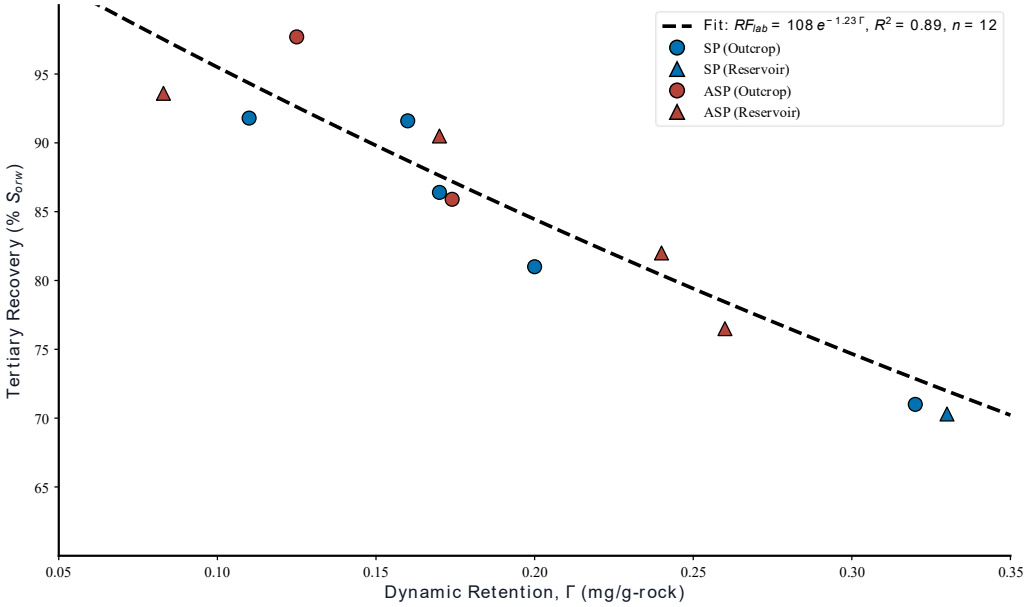

Fig. 2. Empirical relation between dynamic surfactant retention (Γ) and laboratory tertiary oil recovery (RF_{lab}) for the screened GAC/IOS benchmark (n = 12) over the calibrated range Γ = 0.083–0.33 mg/g-rock.

$$RF_{lab} \approx 108 \times \exp(-1.23\,\Gamma) \qquad (2)$$

Over the 12-point calibration set (Table 1), a nonlinear least-squares fit yields R^2 = 0.90, root-mean-square error (RMSE) = 3.0% S_{orw}, and 95% confidence intervals of 101.9–115.2 on the pre-exponential coefficient and −1.60 to −0.97 on the decay constant. The maximum absolute residual is 5.3% S_{orw} (Maubert et al., 2018, CF-1), and the mean absolute residual is 2.3% S_{orw}. These statistics apply to the screened upper-bound subset; prediction intervals for non-optimized systems would be wider. Coefficients in Eq. (2) were obtained by log-linearized ordinary least squares on ln(RF_lab) versus Γ; a nonlinear least-squares refit on the untransformed data gives a = 108.5 and b = −1.28, within the 95% confidence intervals reported above.

An exponential form was selected because surfactant-bank propagation logic predicts multiplicative recovery loss with retention (Lake et al., 2014); linear and power-law fits on the same dataset yield comparable R^2 values but lack the physical-boundary behavior of an exponential at low Γ.

This relation is an empirical fit to the screened benchmark only. It must not be extrapolated outside the calibrated Γ range, and as Γ approaches zero, the fit approaches an unphysical 108%, necessitating a strict upper physical boundary of 100% of S_{orw}. The fit is therefore used here as a compact screening description of the optimized laboratory subset. Because the present framework does not include explicit surfactant-bank propagation or active-mass depletion modeling, high-Γ cases are treated only as bounded screening stress cases within the calibrated subset.

3.3. Contextual Operability Evidence from Kuwait, the UAE, and Oman

Contextual evidence from Kuwait, the UAE, and Oman is retained only to constrain operability, not to calibrate the economic transform. Across these cases, reservoir conditions span approximately 78–100 °C and 180,000–235,000 ppm TDS. In Kuwait, the SAMA multi-well ASP pilot achieved an average oil-cut uplift of approximately 12 percentage points sustained over six months, with a central-producer rate increasing by a factor of 2.0 (Al-Murayri et al., 2022). In the corresponding single-well chemical tracer (SWCT) program, residual oil saturation (S_{orw}) decreased to approximately 0.04 (Carlisle et al., 2014). In the UAE, an offshore one-spot SP test confirmed in-situ residual-oil mobilization via a post-CEOR SWCT, reducing S_{or} to approximately 4%, despite injectivity constraints (Al-Amrie et al., 2015). Finally, in Oman, Upper Shuaiba continuous-injection trials demonstrated measurable field oil gain, though post-review testing indicated reduced recovery once injection-water salinity drifted past a threshold of approximately 150,000 ppm TDS (Wang et al., 2024; Karpan et al., 2025). Collectively, the cases show that residual-oil response can be observed under HTHS carbonate conditions, but execution remains highly sensitive to injectivity management, salinity control, conformance, mobility control, and surveillance. These cases narrow uncertainty around operability but do not validate Eq. (2), E_v, S_{orw}/S_{oi}, or the assumed production timing in the DCF model.

4. Techno-economic Screening Framework and Retention-Driven Value Sensitivity

Section 4 applies a deterministic techno-economic screening model to examine how selected technical and economic assumptions affect project value for a representative HTHS carbonate case. The model is scenario-based and is intended for comparative screening rather than field prediction. The overall workflow linking the screened benchmark to the discounted-cash-flow outputs is summarized in Fig. 11 (presented at the end of Section 4).

4.1. Screening Basis and Assumptions

The economic model evaluates a brownfield expansion of a representative Middle Eastern carbonate sector. The analysis is conducted using a 6-year total project timeline (Year 0 capital expenditure (CAPEX), Years 1–5 Operations), with all costs and revenues expressed in constant 2026 USD.

This discounted cash flow (DCF) model uses pre-tax cash flows for incremental production. It excludes royalties, income taxes, fiscal terms, and financing. It reports results in constant 2026 USD under a flat oil price deck.

4.1.1. Reservoir and Pattern Basis

Representative reservoir and project inputs function as literature-anchored screening variables rather than as field-calibrated constants (Table 2). The objective is to define a bounded base case consistent with the reservoir quality, fluid properties, saturation state, sweep limitations, and brownfield development context reported for HTHS carbonate applications.

Although the field and pilot cases described in Section 3.3 are not used to calibrate Eq. (2) or the production schedule, their reported reservoir properties inform the selection of screening-input ranges in this section. This distinction preserves the separation between operability context and calibration data: the field cases anchor the plausible input space for the DCF model without serving as calibration data for the retention–recovery correlation.

A porosity of $\phi = 0.20$ serves as the base-case screening value. This is consistent with the 0.18–0.30 porosity range reported for the SAMA carbonate system and with the 20–25% porosity reported for the Abu Dhabi offshore Lower Cretaceous CEOR target interval (Carlisle et al., 2014; Al-Amrie et al., 2015; Al-Murayri et al., 2022).

Oil formation volume factor was treated using a literature-anchored Middle Eastern carbonate range rather than a generic PVT default. Reported values include $B_o = 1.16$ RB/STB for the SAMA bottomhole sample, $B_o = 1.14$ RB/STB for the corresponding reconstituted live oil, and $B_o = 1.322$ RB/STB at saturation pressure for the Abu Dhabi offshore carbonate CEOR pilot. Accordingly, $B_o = 1.25$ RB/STB was adopted as a representative mid-range screening value (Al-Amrie et al., 2015; Al-Murayri et al., 2017).

Initial oil saturations (S_{oi}) of 0.70–0.80 and post-waterflood residual oil saturations (S_{orw}) of about 0.35–0.40 are representative of the more residual-oil-rich cases relevant to screening. Accordingly, $S_{orw}/S_{oi} = 0.50$ was adopted. This value was anchored to $S_{orw} = 0.35$ and $S_{oi} = 0.70$, which give $S_{orw}/S_{oi} = 0.50$. Sensitivity was restricted to 0.45–0.55 (±10% around the base case) to test moderately lower and higher residual-oil cases around that pilot-grounded base case without expanding the economic screen to the full saturation envelope reported across all studies (Carlisle et al., 2014; Jabbar et al., 2017; Al-Murayri et al., 2022).

Volumetric sweep efficiency was treated as a literature-informed screening variable rather than as a measured field constant. The cited carbonate literature indicates that contacted volume is limited by heterogeneity, breakthrough, and conformance effects, while polymer and diversion measures may improve sweep relative to an unmanaged flood. Accordingly, $E_v = 0.55$ was adopted as the base case and varied over 0.50–0.60 in sensitivity analysis. This range is intended to represent moderately less favorable and moderately improved sweep outcomes within the same carbonate screening framework rather than a direct field measurement of sweep efficiency (Carlisle et al., 2014; Jabbar et al., 2017; Al-Murayri et al., 2022).

Brownfield facilities CAPEX was treated as a scenario-based screening variable. The cited carbonate CEOR literature indicates that offshore deployment requires dedicated chemical-handling and topside modifications, while broader chemical-EOR cost studies show that existing infrastructure and water-treatment scale can materially moderate brownfield facilities cost. Accordingly, a mid-range brownfield CAPEX of 25 MMUSD was adopted, with a sensitivity range of 20–30 MMUSD intended to bracket lower-scope tie-in cases and cases requiring broader topside modification and chemical-handling scope (Henthorne et al., 2014; Al-Amrie et al., 2015; Morel et al., 2016).

Table 2. Reservoir and operational inputs under the screening model assumptions

Parameter	Value	Unit	Rationale
OOIP	15.0	MMstb	4-pattern sector module (5-spot)
Porosity ϕ	0.20	fraction	Base-case screening value
Initial Oil Saturation S_{oi}	0.70	fraction	Screening basis
Residual Oil Saturation S_{orw}	0.35	fraction	Screening basis
Residual-oil scaling ratio S_{orw}/S_{oi}	0.50	fraction	Pilot-grounded screening assumption
Oil formation volume factor (B_o)	1.25	RB/STB	Mid-range literature-grounded screening value
Sector PV (4 Patterns)	26.79	MMbbl	Calculated
Total Injection	1.2	PV	0.3 ASP + 0.1 PD1 + 0.8 PD2
Volumetric Sweep Efficiency E_v	0.55	fraction	Mid-range carbonate screening assumption
Duration	5.0	years	4,400 bpd per pattern (17,600 bpd total sector injection rate across 4 five-spot patterns)
Base Oil Price	60.0	USD/bbl	Conservative screening threshold below consensus (World Bank, 2025; U.S. EIA, 2026)
Discount Rate	10.0	%	Industry-standard for upstream project evaluation (Harden, 2014)
CAPEX	25.0	MMUSD	Mid-range value for brownfield development
OPEX (Total Injection)	0.94	USD/bbl	Including water softening
OPEX (Total Production)	5.0	USD/bbl	This cost is charged per barrel of incremental oil

Note: *1 stb or bbl = 0.158987 m³. Accordingly, OOIP = 15.0 MMstb corresponds to 2.385 × 10⁶ m³, sector PV = 26.79 MMbbl corresponds to 4.260 × 10⁶ m³, and* B_o reported in RB/STB is numerically equivalent to m³/m³.

4.1.2. Injection and Sweep Basis

The staged ASP, Polymer Drive 1 (PD1), and Polymer Drive 2 (PD2) sequence is used here only as a literature-grounded costing basis for screening (Al-Murayri et al., 2022; Jabbar et al., 2017; Al-Murayri et al., 2017). It represents a chemically active slug followed by a transition/polymer drive and a polymer chase to preserve mobility support. The specific stage sizes and concentrations reported in Table 3 are retained only to parameterize fixed chemical spend in the DCF model; they are not presented as a transport-optimized field recipe. In the present framework, volumetric sweep efficiency remains an external screening variable, and the staged formulation should therefore be interpreted as a representative cost basis rather than as a field-ready design.

4.1.3. Screening Transform from Laboratory Recovery to Field Screening Recovery

The key linkage between the laboratory benchmark and the economic model is the empirical correlation in Section 3.2. Applying assumed constants $E_v = 0.55$ and $S_{orw}/S_{oi} = 0.50$ yields a scenario-specific field-screening transform for the selected case. This transform is a screening construct under stated assumptions, not a validated field-prediction equation.

$$RF_{field}\ (\%\ \mathrm{OOIP}) = RF_{lab} \times E_v \times (S_{orw} / S_{oi}) = 108 \times E_v \times (S_{orw} / S_{oi}) \times \exp(-1.23\,\Gamma) \approx 29.7 \times \exp(-1.23\,\Gamma) \quad (3)$$

In the present model, injected chemical volumes, chemical concentrations, and total chemical spend are held constant across Γ cases. Accordingly, Γ affects economics through the modeled change in incremental recovery and therefore through revenue, UTC, and NPV_{10}. The fixed-spend setup is useful for screening, but it likely understates the full penalty of high retention in field execution because additional active surfactant mass would ordinarily be required to maintain bank integrity. As a bounding estimate, if active surfactant mass were scaled linearly with Γ to maintain constant bank concentration at the flood front, total chemical cost at $\Gamma = 0.30$ mg/g-rock would increase by roughly 50% relative to the $\Gamma = 0.20$ base case, shifting NPV_{10} from −9.7 to approximately −39 MMUSD. The fixed-spend outputs should therefore be read as conservative penalty estimates for the high-retention cases.

4.1.4. Schedule and Timing Assumptions

The operational schedule uses a simplified 5-year response profile with early cash generation for the base screening case. This timing is retained only to compare scenarios on a common basis and is not field-calibrated. Because delayed bank development or later production response would reduce discounted value at unchanged total recovery, all NPV_{10} and breakeven outputs should be interpreted as timing-conditional screening results. A one-year delayed-response sensitivity with unchanged total recovery is therefore examined in Fig. 5.

4.1.5. Cost Basis and Chemical Design

The injection strategy employs a total injection volume of 1.20 PV (Table 3). The cost structure reflects a brownfield-expansion context.

Chemical unit costs were selected from published CEOR economics studies, with preference for ASP assumptions that are either directly reported for carbonate applications or consistent with the chemistry used in this work. Surfactant cost is discussed first because it dominates total chemical expenditure and is the main explicitly varied chemical-cost parameter in the sensitivity analysis. For the GAC/IOS system, Al-Murayri et al. (Al-Murayri et al., 2017) reported a manufacturing cost of about 3.31 USD/kg (1.50 USD/lb) at a large commercial scale. A base-case surfactant cost of 4.41 USD/kg (2.00 USD/lb) was therefore adopted as a screening value for a blended GAC/IOS system. This places the base case above the chemistry-specific manufacturing-cost floor while remaining below broader project-level screening values used in CEOR economic studies (Henthorne et al., 2014; Sheng, 2014; Al-Murayri et al., 2017). Sensitivity was evaluated over 3.31–5.51 USD/kg (1.50–2.50 USD/lb).

For the remaining chemicals, polymer was set to 3.86 USD/kg (1.75 USD/lb), alkali to 0.33 USD/kg (0.15 USD/lb), and co-solvent to 1.65 USD/kg (0.75 USD/lb). Polymer was varied over 3.09–4.63 USD/kg (1.40–2.10 USD/lb), alkali over 0.26–0.40 USD/kg (0.12–0.18 USD/lb), and co-solvent over 1.32–1.98 USD/kg (0.60–0.90 USD/lb). These ranges were used as practical screening intervals around the selected base-case values rather than as transferable procurement prices (Henthorne et al., 2014; Sheng, 2014; Al-Murayri et al., 2017).

A uniform ±20% sensitivity was applied to the non-surfactant cost components as a practical screening rule to represent procurement and formulation-cost uncertainty without implying unwarranted pricing precision (Henthorne et al., 2014; Sheng, 2014).

Variable production operating expenditure (OPEX) is 5.00 USD/bbl of incremental oil, covering incremental lifting, separation, dehydration, and produced-water handling. This variable cost allowance reflects the incremental burden of emulsion treatment and produced-water management that accompanies surfactant flooding, where emulsion destruction and treatment add to the overall production cost and must be considered alongside displacement economics (Yonguep et al., 2022). Total injection OPEX is 0.94 USD/bbl injected, comprising a base injection cost of 0.87 USD/bbl plus a water-treatment allocation. An additional 0.07 USD/bbl injected is included for brownfield chemical-handling requirements (Henthorne et al., 2014).

Table 3 defines the chemical-cost screening inputs and staged formulation basis used in the fixed-spend economic model. The unit costs are intended as literature-grounded screening values rather than field-calibrated procurement prices. The surfactant lower bound is chemistry-specific, the co-solvent cost remains a screening allowance, and the PD1/PD2 stages are retained to preserve published carbonate trailing-edge conditioning and mobility-control logic rather than to reproduce any single field recipe exactly.

Table 3. Chemical-cost screening inputs and graded formulation basis used in the economic model

Component / stage	Base case	Sensitivity range	Basis
Surfactant	2.00 USD/lb	1.50–2.50 USD/lb	1.50 USD/lb chemistry-specific manufacturing anchor for GAC/IOS; 2.00 USD/lb adopted as the screening base case for the blended system; broader project-level screening values extend above this base case (Henthorne et al., 2014; Al-Murayri et al., 2017; Sheng, 2014)
Polymer	1.75 USD/lb	1.40–2.10 USD/lb	Screening base case anchored to ASP economics and polymer-cost literature (Henthorne et al., 2014; Sheng, 2014)
Alkali (Na_2CO_3-basis)	0.15 USD/lb	0.12–0.18 USD/lb	Screening base case anchored to ASP economics and commodity alkali cost literature (Henthorne et al., 2014; Sheng, 2014)
Co-solvent (ethoxylated phenol basis)	0.75 USD/lb	0.60–0.90 USD/lb	Screening allowance consistent with published ASP usage; transferable project pricing is not established in the cited literature (Henthorne et al., 2014; Al-Murayri et al., 2017; Sheng, 2014)
ASP slug	0.30 PV	fixed in base formulation	1.0 wt% surfactant, 1.0 wt% alkali, 0.5 wt% co-solvent, 2800 ppm polymer
PD1	0.10 PV	fixed in base formulation	0.2 wt% alkali, 0.5 wt% co-solvent, 2500 ppm polymer

Component / stage	Base case	Sensitivity range	Basis
PD2	0.80 PV	fixed in base formulation	2000 ppm polymer only

Note: *1 USD/lb = 2.2046 USD/kg. Concentrations reported in wt% and ppm are retained as reported in the source designs and supporting studies.*

4.1.6. Price and Discounting Assumptions

A Brent price of 60 USD/bbl was adopted as a conservative screening threshold, intentionally positioned below the 2025–2030 consensus range of the World Bank Commodity Outlook and U.S. EIA Annual Energy Outlook to provide a stress-test baseline rather than a forecasted price (World Bank, 2025; U.S. EIA, 2026). A 10% real discount rate, consistent with industry-standard upstream project evaluation (Harden, 2014), was paired with this price deck. Together, these assumptions define a bounded screening basis in which the base case is biased toward understatement of value; favorable outcomes under this conservative deck would strengthen, not weaken, at higher realized prices.

4.2. Base-case Screening Results

The base case is defined by Γ = 0.20 mg/g-rock, Brent = 60 USD/bbl, E_v = 0.55, surfactant cost = 4.41 USD/kg (2.00 USD/lb), CAPEX = 25 MMUSD, and real discount rate = 10.0%.

4.2.1. Cost Structure and Value Drivers

Under the fixed-spend formulation used here, Table 4 reports the cost composition of the base chemical design for the base-case screening scenario. Under the base-case assumptions, the modeled field recovery factor is 23.2% OOIP, yielding 3.48 MMstb of incremental oil and gross revenue of 209.0 MMUSD. Surfactant and polymer remain the dominant contributors to total chemical expenditure.

Table 4. Chemical cost distribution and project capital allocation under the base-case screening assumptions.

A. Chemical Cost Breakdown		
Cost Component	**Cost (MMUSD)**	**Share (%)**
Surfactant	56.26	47.3
Polymer	44.14	37.1
Co-solvent	14.06	11.8
Alkali	4.50	3.8
Total chemical cost	**118.96**	**100.0**

B. Overall Project Cost Allocation	
Cost Category	**Cost (MMUSD)**
Injection OPEX (non-chemical)	30.22
Production OPEX (variable)	17.42
Facilities CAPEX (brownfield)	25.00
Total project cost (undiscounted)	**191.60**

With the injected formulation and spend held constant across the Γ cases, higher retention worsens the chemical cost per incremental barrel by reducing the modeled incremental oil. Fig. 3, therefore, shows a per-barrel cost response under fixed total spend rather than evidence that higher retention increases total chemical spend.

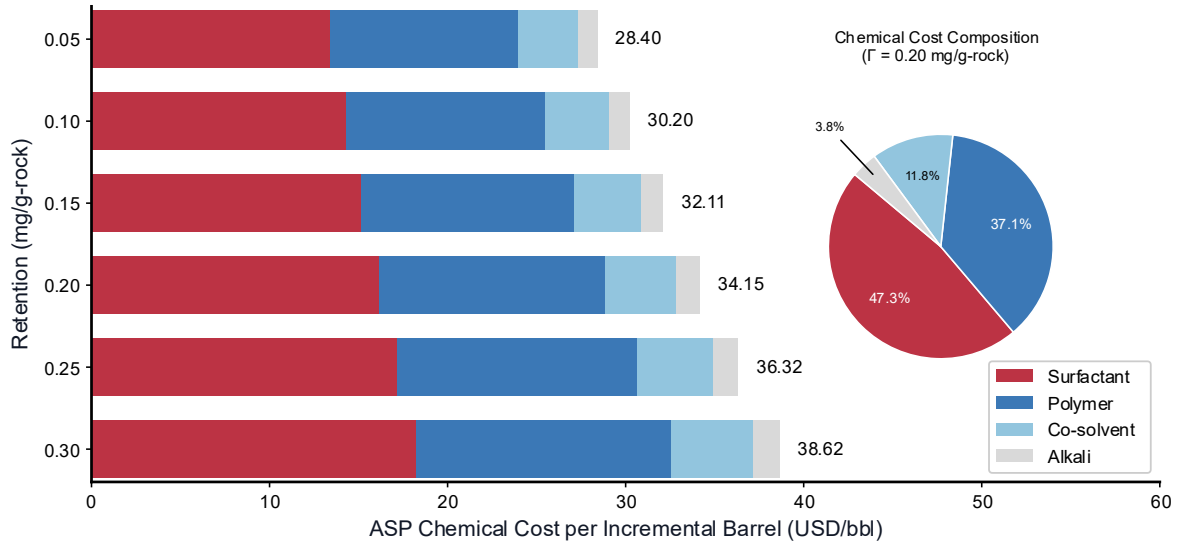

Fig. 3. Chemical cost breakdown per incremental barrel as a function of dynamic retention (Γ) under the fixed-spend screening formulation.

4.2.2. Base-case Outputs and Resource Intensity

Under the base-case screening assumptions (Γ = 0.20 mg/g-rock, Brent = 60 USD/bbl, E_v = 0.55, CAPEX = 25 MMUSD, real discount rate = 10%), the model gives NPV_{10} = 7.2 MMUSD, IRR = 20.7%, UTC = 55.0 USD/bbl, $RF_{field} \approx$ 23.2% OOIP, incremental oil ≈ 3.48 MMstb, and gross revenue of 209.0 MMUSD. Total chemical cost under the fixed-spend formulation is 119.0 MMUSD, corresponding to a chemical cost of 34.2 USD/bbl of incremental oil. At the base surfactant price of 4.41 USD/kg (2.00 USD/lb), the fixed-spend design implies an active-surfactant intensity of 23.05 kg per incremental m³ (8.08 lb/bbl).

Table 5 summarizes the DCF outputs as a function of dynamic retention under the base oil-price case of 60 USD/bbl.

Table 5. DCF model outputs and active-surfactant intensity metric as a function of dynamic retention (Γ) at 60 USD/bbl

Γ (mg/g-rock)	NPV_{10} (MMUSD)	IRR (%)	Chem Cost (USD/bbl)	UTC (USD/bbl)	Surfactant Intensity, kg/m³ (lb/bbl)	Status
0.083	29.6	50.1	29.57	48.30	19.94 (6.99)	Favorable
0.10	26.2	45.8	30.20	49.22	20.37 (7.14)	Favorable
0.15	16.4	33.3	32.11	52.02	21.65 (7.59)	Favorable
0.20	7.2	20.7	34.15	55.00	23.05 (8.08)	Viable (Base case)
0.25	−1.5	7.6	36.32	58.17	24.51 (8.59)	Uneconomic
0.30	−9.7	< 0[a]	38.62	61.55	26.04 (9.13)	Uneconomic
0.32	−12.8	< 0[a]	39.58	62.96	26.70 (9.36)	Uneconomic

Note: *1 USD/bbl = 6.2898 USD/m³ and 1 lb/bbl = 2.8530 kg/m³. [a] IRR is reported as "< 0" when total undiscounted net cash flow is negative, indicating that no positive real discount rate yields NPV = 0.*

The table shows how higher retention reduces modeled recovery and value while increasing unit technical cost under the fixed-spend screening formulation. Values outside the calibrated benchmark range should be read as screening stress cases rather than calibrated outcomes.

Fig. 4 recasts the same retention cases in operational-efficiency terms by reporting active surfactant intensity per incremental barrel. Here, active surfactant intensity is defined as total injected active surfactant mass divided by incremental oil, reported in kg/m³ (lb/bbl). Because the fixed-spend screening model holds injected active surfactant mass constant across Γ cases, the metric increases monotonically with retention only because modeled incremental oil declines under the retained laboratory-to-field screening transform (Henthorne et al., 2014; Sheng, 2014; Al-Murayri et al., 2017).

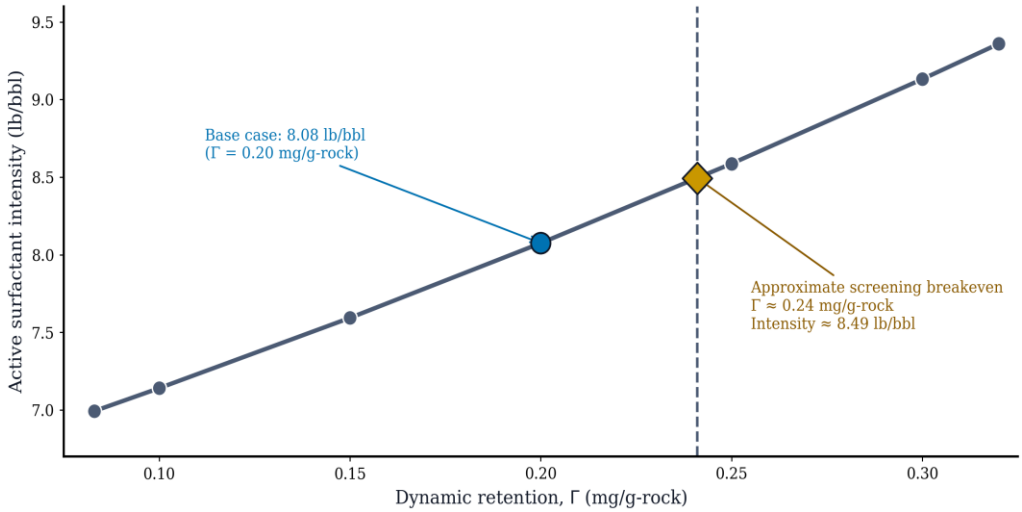

Fig. 4. Active surfactant intensity per incremental barrel as a function of dynamic retention (*Γ*) under the fixed-spend screening formulation.

At the base case, the active surfactant intensity is 23.05 kg/m³ (8.08 lb/bbl) at Γ = 0.20 mg/g-rock. The metric declines to about 19.94–21.65 kg/m³ (6.99–7.59 lb/bbl) in the lower-retention cases and rises to about 24.51–26.70 kg/m³ (8.59–9.36 lb/bbl) in the higher-retention screening cases, providing a compact resource-intensity complement to NPV and UTC under the same fixed-spend assumptions (Henthorne et al., 2014; Sheng, 2014; Al-Murayri et al., 2017).

4.2.3. Timing Sensitivity

Fig. 5 compares the base discounted-cash-flow profile with a one-year delayed-response sensitivity in which total recovery is held constant and cash-flow realization is shifted by one year. Under that timing-only stress case, NPV_{10} decreases from 7.2 to 4.2 MMUSD and IRR decreases from 20.7% to 14.7%.

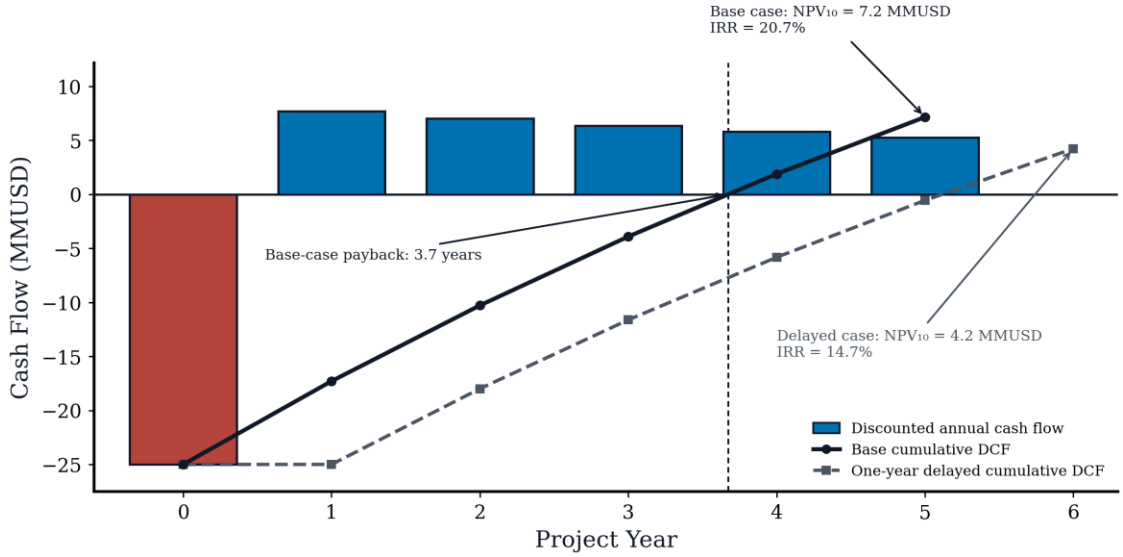

Fig. 5. Discounted cash flow (DCF) profile showing annual discounted net cash flow, the base-case cumulative discounted cash flow, and a one-year delayed-response sensitivity with unchanged total recovery.

The delayed case lowers discounted value without changing total modeled recovery, confirming that the quoted breakeven outputs remain conditional on the assumed early-response schedule rather than on a field-calibrated production profile.

4.3. Sensitivity Ranking and Viability Envelope

Figs. 6–9 and Table 6 summarize the synchronized economic outputs generated from the scenario-based screening model. Within the tested one-at-a-time ranges, retention is the dominant driver, followed by saturation-state and sweep assumptions; oil

price and surfactant cost remain material but smaller. The oil-price/retention outputs are presented as scenario-specific screening results, and the 50 USD/bbl case provides a downside screening case under the same assumptions.

4.3.1. Tornado Analysis: Ranking of Economic Uncertainties

Fig. 6 ranks the one-at-a-time sensitivity of each screened parameter by its effect on NPV_{10} relative to the base case of 7.2 MMUSD. The parameters are grouped into three uncertainty categories – subsurface (technical), operational (cost), and macro-financial (external) – to clarify which risk class drives the screening outcome and where targeted data acquisition yields the largest reduction in economic uncertainty.

Among the subsurface (technical) parameters, retention (Γ) exerts the widest swing of any single parameter (−19.9 to +22.5 MMUSD), consistent with the nonlinear exponential dependence of incremental recovery on Γ through Eq. (2). The bar is asymmetric: reducing Γ from 0.20 to 0.083 mg/g-rock adds 22.5 MMUSD because the exponential steepens at lower retention, whereas increasing Γ to 0.32 mg/g-rock subtracts only 19.9 MMUSD because the curve flattens at higher retention. The S_{orw}/S_{oi} ratio (±14.5 MMUSD) ranks second and reflects uncertainty in the initial saturation state and waterflood efficiency of the target zone. Volumetric sweep efficiency E_v (±13.2 MMUSD) produces a symmetric bar of similar magnitude because incremental recovery scales linearly with E_v. Together, these three subsurface parameters account for the dominant share of total NPV uncertainty, which means that coreflood retention measurement, saturation characterization, and conformance assessment are the highest-value technical activities for narrowing the screening envelope prior to pilot consideration.

The operational (cost) parameters occupy the middle tier. Surfactant cost (±10.7 MMUSD over 3.31–5.51 USD/kg (1.50–2.50 USD/lb)) ranks below retention despite being the dominant cost component, because the fixed-spend formulation holds total injected volume constant and surfactant cost affects only the per-barrel chemical charge. Other chemical costs (±9.5 MMUSD under ±20% variation) capture combined uncertainty in polymer, alkali, and co-solvent pricing. CAPEX (±5.0 MMUSD over 20–30 MMUSD) reflects brownfield scope variation. These cost parameters are contractual or engineering-design variables that can be refined through procurement and front-end engineering without additional subsurface data.

The macro-financial (external) parameters exert the smallest and largest bounded effects depending on whether the range represents base-case uncertainty or full scenario variation. The oil-price bar in Fig. 6 reflects a ±5 USD/bbl variation around the 60 USD/bbl screening price to represent uncertainty in the selected base-case assumption (±13.2 MMUSD); broader oil-price scenarios (50–70 USD/bbl) are examined separately in the response surface (Fig. 8) and the full sensitivity matrix (Table 6). Discount rate (−1.6 to +1.7 MMUSD over 8–12%) exerts the smallest effect of any tested parameter because the 5-year project horizon limits the compounding window. Under the stated screening assumptions, the model indicates an approximate breakeven oil price of 57.3 USD/bbl at Γ = 0.20 mg/g-rock and an approximate breakeven retention of 0.24 mg/g-rock at 60 USD/bbl.

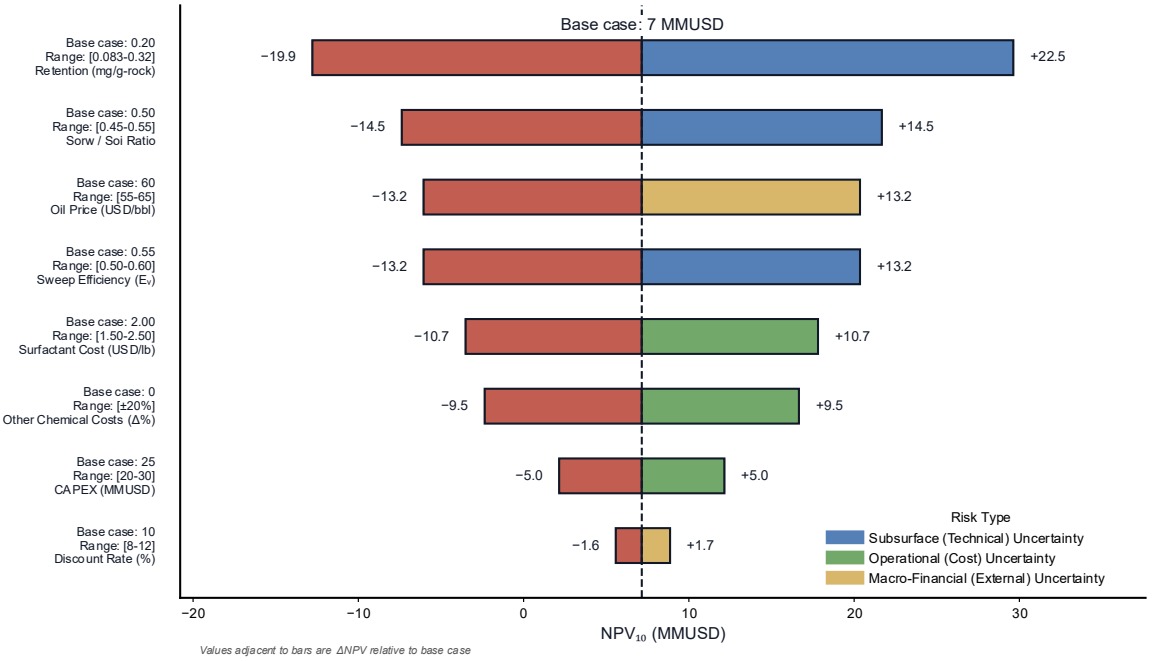

Fig. 6. Tornado sensitivity analysis of project NPV at a 10% real discount rate, grouped by subsurface (technical), operational (cost), and macro-financial (external) uncertainty classes.

4.3.2. Sweep Efficiency Sensitivity

Fig. 7 shows an approximately linear NPV response to volumetric sweep efficiency in the present screening model because incremental recovery scales directly with E_v while the other major assumptions are held fixed. The base case at $E_v = 0.55$ gives $NPV_{10} = 7.2$ MMUSD, while the approximate breakeven sweep efficiency is $E_v \approx 0.523$ under the stated assumptions.

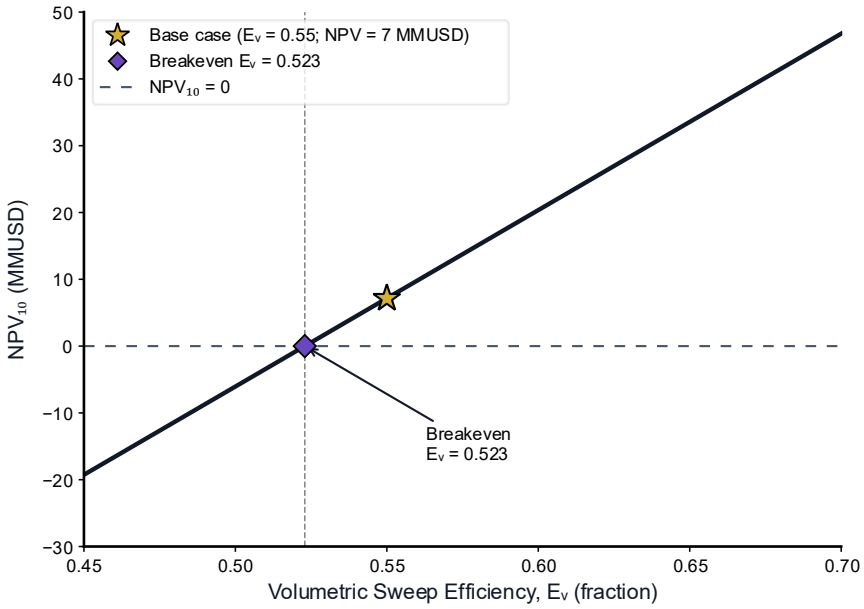

Fig. 7. Sensitivity of project NPV to volumetric sweep efficiency (E_v).

4.3.3. Economic Response Surface and Limits

Fig. 8 presents the screening-model response surface in oil-price/retention space. Positive NPV occurs at lower retention and higher oil price, while the dashed contour marks the approximate scenario-specific breakeven boundary. Cases beyond that modeled boundary are more appropriately interpreted as requiring reformulation, lower CAPEX, or revised operating assumptions before further consideration.

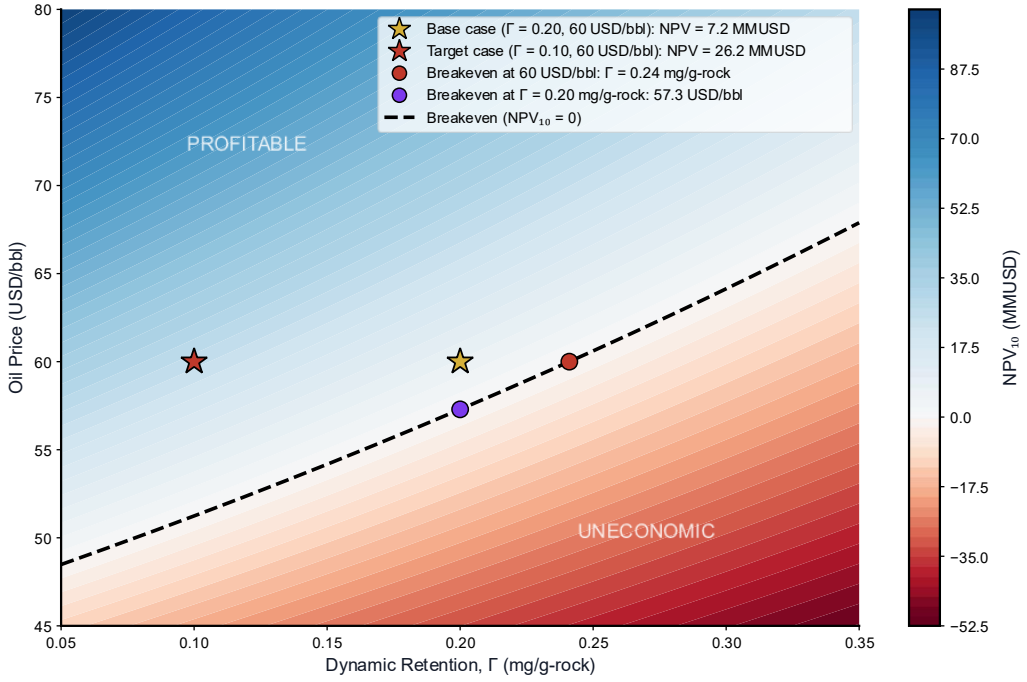

Fig. 8. Screening-model economic response surface of NPV versus oil price and dynamic retention (Γ).

Fig. 9 resolves the boundary interpretation by showing panel (a) the approximate breakeven oil price as a function of Γ and panel (b) the chemical cost per incremental barrel under the fixed-spend formulation. The base case at Γ = 0.20 mg/g-rock remains inside the positive-NPV region at 60 USD/bbl, whereas the approximate breakeven limit occurs near Γ ≈ 0.24 mg/g-rock.

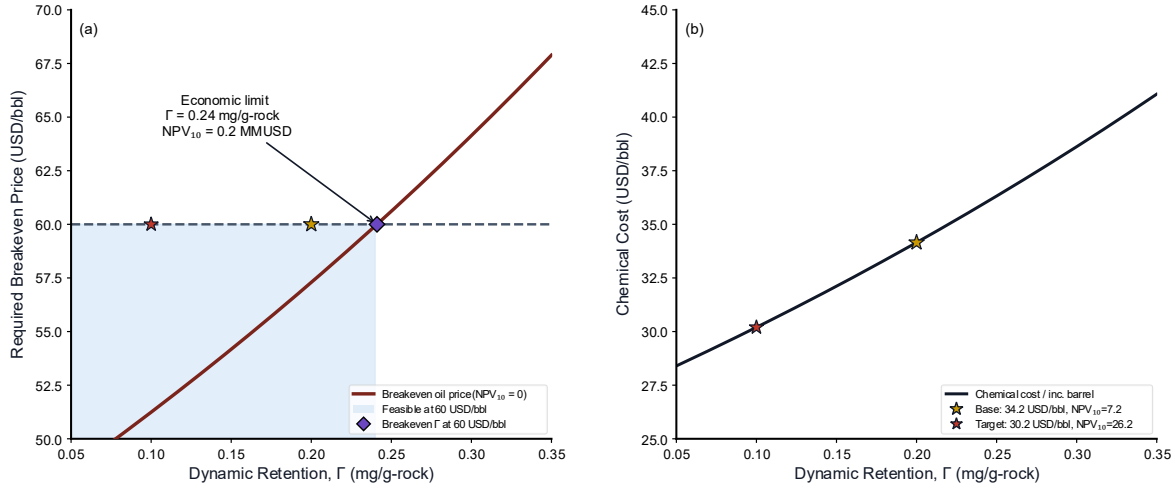

Fig. 9. Screening-model envelope: (a) approximate breakeven oil price at NPV_{10} = 0 versus dynamic retention (Γ); and (b) chemical cost per incremental barrel versus Γ under the fixed-spend screening formulation.

Table 6 presents the full NPV sensitivity matrix across oil price and retention under the stated screening assumptions.

Table 6. NPV_{10} sensitivity matrix (MMUSD)

Γ (mg/g-rock)	50 USD/bbl	55 USD/bbl	60 USD/bbl	65 USD/bbl	70 USD/bbl
0.083	−0.9	14.4	29.6	44.9	60.1
0.10	−3.7	11.2	26.2	41.1	56.0
0.15	−11.7	2.3	16.4	30.4	44.5
0.20	−19.3	−6.1	7.2	20.4	33.6
0.25	−26.3	−13.9	−1.5	10.9	23.3
0.30	−33.0	−21.3	−9.7	2.0	13.7
0.32	−35.6	−24.2	−12.8	-1.4	10.0

Within Table 6, the positive-NPV region at 60 USD/bbl extends from $\Gamma = 0.08$ to 0.20 mg/g-rock, with approximate breakeven near $\Gamma \approx 0.24$ mg/g-rock under the stated assumptions. At 50 USD/bbl, all tested retention cases yield negative NPV. At $\Gamma = 0.30$ mg/g-rock, the matrix implies that an oil price above 65 USD/bbl would be required to reach breakeven under the same assumptions. Cases outside the calibrated benchmark range should be interpreted as screening stress cases.

4.3.4. Stress Test: The 50 USD/bbl Scenario

Under the 50 USD/bbl stress scenario, all tested retention cases yield negative NPV under the stated assumptions. The lowest-retention case ($\Gamma = 0.08$ mg/g-rock) gives $NPV_{10} \approx -0.9$ MMUSD, while the base-case retention of $\Gamma = 0.20$ mg/g-rock gives $NPV_{10} = -19.3$ MMUSD. CAPEX compression alone from 25 to 20 MMUSD is insufficient to restore positive NPV at $\Gamma = 0.20$ mg/g-rock. A viable low-price case would require either substantial retention reduction or combined retention, CAPEX, and chemical-cost improvement.

4.4. Updating the Screen with Improved Technical Information

4.4.1. Sweep Efficiency and Retention Improvement Envelope

The base case yields positive NPV (NPV_{10} = +7.2 MMUSD) but remains sensitive to downside risks. Two changes drive the largest NPV increase in this screening model: improving volumetric sweep efficiency and reducing surfactant retention. If sweep efficiency is increased to 0.60, NPV_{10} increases to 20.4 MMUSD. If retention is independently reduced to 0.10 mg/g-rock, NPV_{10} increases to 26.2 MMUSD.

The waterfall (Fig. 10) decomposes the NPV increase when E_v and Γ change sequentially. Increasing E_v from 0.55 to 0.60 raises NPV by 13.2 MMUSD, while subsequently lowering retention to 0.10 mg/g-rock adds a further 20.7 MMUSD, yielding an optimized project NPV of 41.1 MMUSD.

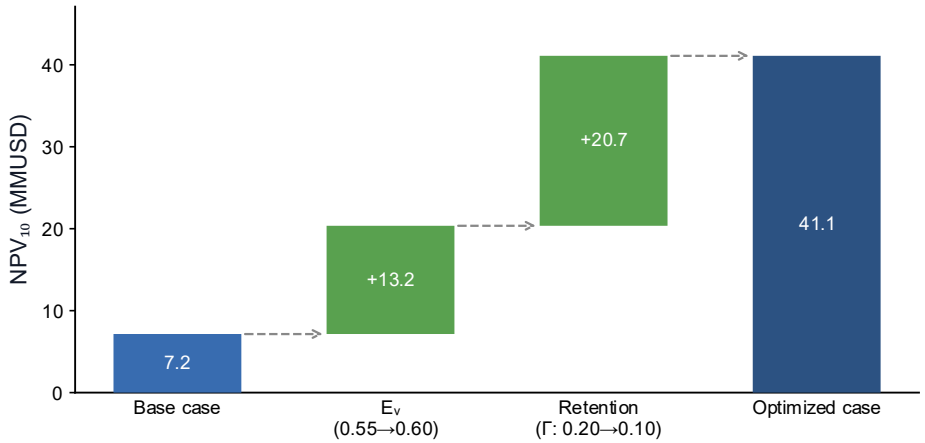

Fig. 10. Incremental NPV sensitivity to sweep efficiency (E_v) and dynamic retention (Γ) improvements.

This waterfall view shows that retention reduction contributes 20.7 MMUSD out of a total 33.9 MMUSD NPV gain from the base case to the optimized case, which is about 61% of the total gain. Within the tested screening ranges, retention and sweep efficiency contribute the largest share of the modeled NPV increase under the stated cost structure.

4.4.2. Pilot Updating of Screening Assumptions

Given the sensitivity of the screening outputs to Γ, E_v, CAPEX, and timing assumptions, any pilot evaluation should test whether field-scale retention and sweep remain within the modeled screening ranges. If pilot data indicate materially higher retention, lower sweep, or slower production response than assumed here, the economic screen should be rerun with revised inputs before further scale-up decisions are made.

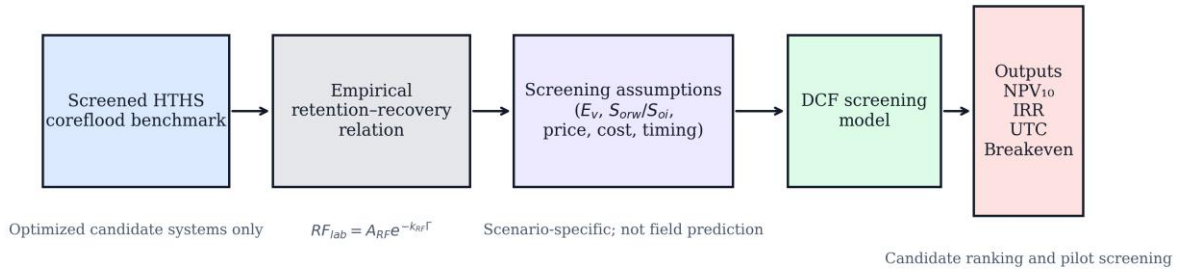

Fig. 11. Workflow of the techno-economic screening framework linking the screened benchmark to the scenario-based DCF outputs.

4.4.3. Framework Self-Check Against Contextual Pilot Data

To assess whether the screening framework produces field-plausible outputs, Eq. (3) is applied to conditions approximating the Kuwait SAMA ASP pilot (Al-Murayri et al., 2022; Carlisle et al., 2014). This is not a calibration exercise — retention for the SAMA formulation is not independently reported on the same basis as Table 1 — but it tests whether the screening transform produces recovery estimates within the order of magnitude reported for the field response.

Using the benchmark mid-range $\Gamma = 0.20$ mg/g-rock and a plausible composite $E_v \times (S_{orw}/S_{oi})$ near 0.20 (representative of a moderately contacted pilot pattern), Eq. (3) gives RF_{field} of order 20% OOIP at the screening transform. The SAMA pilot reported an oil-cut uplift of approximately 12 percentage points sustained over six months with a doubling of central-producer rate, consistent with an incremental recovery in the high single-digit to low double-digit OOIP range under reasonable contacted-volume assumptions. The framework output falls within the order-of-magnitude envelope of the observed field response, supporting use of the screening transform for candidate ranking.

This order-of-magnitude agreement is not a validation of Eq. (3) — SAMA formulation retention is not measured on the same basis as the Table 1 benchmark, and pilot contacted volume is not a screening output — but the agreement suggests the framework is not systematically biased at base-case conditions.

5. Limitations

The empirical Γ–RF_{lab} relationship is calibrated only on n = 12 laboratory observations over Γ = 0.083–0.33 mg/g-rock and should not be extrapolated outside that range.

The benchmark is a screened upper-bound subset of optimized candidate systems rather than a representative distribution of carbonate CEOR outcomes. The Kuwait, the UAE, and Oman cases provide contextual operability evidence only and are not used to calibrate Eq. (2), E_v, S_{orw}/S_{oi}, or production timing. Because the benchmark is calibrated on screened, optimized systems, the economic outputs likely represent an upper bound on expected project value; application to non-optimized or less favorable formulations would shift the NPV distribution downward.

The empirical fit in Eq. (2) aggregates corefloods across Silurian dolomite, Indiana Limestone, and reservoir carbonate at 78–100 °C, implicitly assuming that lithology and temperature do not systematically shift the retention–recovery relationship within the screened range. This assumption has not been independently tested and may introduce unquantified confounding.

The discounted-cash-flow model is deterministic and pre-tax, and it does not include fiscal terms, explicit uncertainty distributions, surfactant-bank propagation, or a field-calibrated delayed-response model. The manuscript therefore supports candidate ranking and pilot screening within the stated assumptions rather than field prediction or universal design thresholds.

5.1. Practical Implications

Within the screening assumptions used here, three practical implications emerge for HTHS carbonate decision-making. First, coreflood retention measurement delivers a larger NPV uncertainty reduction than incremental phase-behavior screening once $\Gamma <$ 0.20 mg/g-rock is achieved; operators should prioritize retention quantification in pre-pilot workflows. Second, at Brent prices below 55 USD/bbl the economic envelope narrows sharply, with only the lowest-retention cases ($\Gamma \leq$ 0.10 mg/g-rock) remaining competitive under base-case costs; operators should rank surfactant flooding against alternative EOR methods in low-price scenarios rather than treating it as a default option. Third, the largest NPV gains at the screening stage come from combined retention reduction ($\Gamma \rightarrow$ 0.10 mg/g-rock) and sweep improvement ($E_v \rightarrow$ 0.60), which together raise base-case NPV from 7.2 to 41.1 MMUSD; surfactant development and conformance control should therefore be advanced in parallel rather than sequentially.

6. Conclusions

This study introduces a scenario-based techno-economic screen for surfactant flooding in HTHS carbonates, with dynamic surfactant retention (Γ) functioning as an explicit bridge variable between coreflood performance and project economics. The framework is calibrated on an upper-bound benchmark of 12 optimized Guerbet alkoxy carboxylate/internal olefin sulfonate corefloods over Γ = 0.083–0.33 mg/g-rock and is coupled to a deterministic discounted-cash-flow model for a representative brownfield carbonate sector. Contextual field cases from Kuwait, the UAE, and Oman inform operability assumptions but do not calibrate the model.

6.1. Key Findings

1. Empirical retention–recovery relation. Over the calibrated range Γ = 0.083–0.33 mg/g-rock, the screened benchmark follows $RF_{lab} = 108 \times \exp(-1.23\,\Gamma)$ with R^2 = 0.90, RMSE = 3.0% S_{orw}, and maximum absolute residual of 5.3% S_{orw}.

2. Base-case economic outputs. At Γ = 0.20 mg/g-rock and Brent = 60 USD/bbl, the framework gives RF_{field} = 23.2% OOIP, incremental oil = 3.48 MMstb, NPV_{10} = 7.2 MMUSD, IRR = 20.7%, and UTC = 55.0 USD/bbl.

3. Screening breakeven points. Under the stated cost structure, screening breakeven occurs at Γ = 0.24 mg/g-rock (at 60 USD/bbl) and at Brent = 57.3 USD/bbl (at Γ = 0.20 mg/g-rock). Beyond Γ = 0.25 mg/g-rock, the fixed-spend model returns negative NPV_{10} under base-case economics.

4. Hierarchical sensitivity structure. Three-tier ranking of screening uncertainties: (a) Subsurface (dominant): retention (−19.9/+22.5 MMUSD), S_{orw}/S_{oi} (±14.5 MMUSD), E_v (±13.2 MMUSD); (b) Operational (middle): surfactant cost (±10.7 MMUSD), other chemicals (±9.5 MMUSD), CAPEX (±5.0 MMUSD); (c) Macro-financial (lowest): oil price (±13.2 MMUSD over ±5 USD/bbl), discount rate (<±2 MMUSD).

5. Combined optimization potential. Simultaneous reduction of Γ to 0.10 mg/g-rock and improvement of E_v to 0.60 raises NPV_{10} from 7.2 to 41.1 MMUSD, a 5.7× gain that exceeds the sum of individual gains, indicating multiplicative benefit from paired subsurface improvements.

6.2. Recommendations for Future Work

Three data-acquisition priorities would materially tighten the screening envelope developed here:

1. Retention characterization at > 110 °C. The screened benchmark is clustered in 78–100 °C. Extending dynamic retention measurements to 110–130 °C would close the high-temperature data gap identified in Section 2.7 and permit direct screening of Middle East carbonate reservoirs currently outside the calibrated range.

2. Integrated phase-behavior and polymer-rheology screening. Few existing studies report full viscosity profiles, thermal stability, and retention for the same core. A coordinated protocol combining salinity scans, rheometry, and coreflood retention on identical reservoir cores would reduce uncertainty in the $E_v \times (S_{orw}/S_{oi})$ composite term, which the sensitivity analysis identifies as the second-ranked driver.

3. Pilot-scale validation of the screening transform. The framework output $RF_{field} = RF_{lab} \times E_v \times (S_{orw}/S_{oi})$ has not been independently validated against a field response. A 4-pattern HTHS carbonate pilot with documented coreflood retention and SWCT residual-oil measurements would allow direct back-test of Eq. (3) and calibration of delayed-response timing factors.

Framework extensions that would strengthen the decision-support scope include probabilistic NPV distributions replacing single-point deterministic outputs, explicit surfactant-bank propagation modeling for high-Γ cases to replace the fixed-spend approximation, and fiscal-terms coupling to move from pre-tax screening to post-tax project economics.

Nomenclature

Symbols

B_o = Oil formation volume factor, RB/STB
E_v = Volumetric sweep efficiency, fraction
N_c = Capillary number, dimensionless
$N_{c,crit}$ = Critical capillary number for desaturation onset, dimensionless
R = Guerbet hydrophobe carbon number
RF = Recovery factor, fraction of OOIP
RF_{field} = Field-scale recovery factor, % OOIP
RF_{lab} = Laboratory tertiary recovery factor, % of S_{orw} or fraction, as defined
RF_{OOIP} = Reported incremental recovery as a fraction of original oil in place, %
S^* = Optimum salinity, ppm or wt%
S_{oi} = Initial oil saturation, fraction of PV
S_{or} = Residual oil saturation, fraction of PV
S_{orc} = Residual oil saturation after chemical flood, fraction of PV
S_{orw} = Residual oil saturation after waterflood, fraction of PV
v = Darcy velocity, m/s

Greek Letters

Γ = Dynamic surfactant retention, mg/g-rock
μ = Viscosity, mPa·s (cP)
ϕ = Porosity, fraction
σ = Interfacial tension, mN/m

Abbreviations

ASP = Alkali-surfactant-polymer flood
CAPEX = Capital expenditures
CEOR = Chemical enhanced oil recovery
DCF = Discounted cash flow
EO = Ethylene oxide

EOR = Enhanced oil recovery
GAC = Guerbet alkoxy carboxylate surfactant
HTHS = High-temperature, high-salinity
IFT = Interfacial tension
IOS = Internal olefin sulfonate
IRR = Internal rate of return
NPV_{10} = Net present value at 10% real discount rate, MMUSD
OOIP = Original oil in place
OPEX = Operating expenditures
PO = Propylene oxide
PV = Pore volume
SP = Surfactant-polymer
SWCT = Single-well chemical tracer test
TDS = Total dissolved solids
UTC = Unit technical cost, USD/bbl
MMbbl = Million barrels
MMstb = Million stock-tank barrels
MMUSD = Million United States dollars
PD1 = Polymer Drive 1
PD2 = Polymer Drive 2
RB = Reservoir barrel
STB = Stock-tank barrel
wt% = Weight percent

Unit Conversions (Field–SI)

1 bbl = 0.158987 m^3
1 lb = 0.45359 kg
1 USD/lb = 2.2046 USD/kg
1 lb/bbl = 2.8530 kg/m^3
1 USD/bbl = 6.2898 USD/m^3
Oil formation volume factor B_o is reported in RB/STB; dimensionless ratio equivalent to m^3/m^3.
1 mPa·s = 1 cP

Data Availability Statement

The calibration dataset used in Table 1 (12 optimized Guerbet alkoxy carboxylate/internal olefin sulfonate coreflood observations) is compiled entirely from the cited published studies and can be reconstructed from Table 1. The discounted-cash-flow model inputs are documented in Tables 2 and 3 of this manuscript. Supplementary Material includes formulation-context figures (Figs. S1–S3), a model-inputs workbook (Model_Inputs.xlsx), a Python script (Python_code.py) that reproduces the manuscript figures and generates model outputs from the inputs workbook, and a plot-ready model-outputs workbook (Model_Outputs.xlsx). Additional source data are available on request.

References

Abalkhail, N., Liyanage, P.J., Upamali, K.A.N., Pope, G.A., Mohanty, K.K., 2020. Alkaline-Surfactant-Polymer Formulation Development for a HTHS Carbonate Reservoir. J. Pet. Sci. Eng. 191, 107236. https://doi.org/10.1016/j.petrol.2020.107236

Adel, I.A., Al-Shalabi, E.W., Hernandez, A., AlAmeri, W., AlSumaiti, A., Masalmeh, S., 2025. Optimized Guerbet Alkoxy Carboxylate Surfactant Formulations for EOR in Carbonates Under Harsh Conditions. Paper SPE-225503-MS. https://doi.org/10.2118/225503-MS

Adkins, S., Liyanage, P.J., Arachchilage, G.P., Mudiyanselage, T., Weerasooriya, U., Pope, G.A., 2012. Development of Thermally and Chemically Stable Large-Hydrophobe Alkoxy Carboxylate Surfactants. Paper SPE-154256-MS. https://doi.org/10.2118/154256-MS

Al-Amrie, O., Peltier, S., Pearce, A., Al-Yafei, A., Morel, D., Bourrel, M., Bursaux, R., Cordelier, P., Jouenne, S., Juilla, H., Klimenko, A., Levitt, D., Nguyen, M., 2015. The First Successful Chemical EOR Pilot in the UAE. Paper SPE-177514-MS. https://doi.org/10.2118/177514-MS

Al-Murayri, M.T., Kamal, D.S., Suniga, P., Fortenberry, R., Britton, C., Pope, G.A., Liyanage, P.J., Jang, S.H., Upamali, K.A.N., 2017. Improving ASP Performance in Carbonate Reservoir Rocks Using Hybrid-Alkali. Paper SPE-187213-MS. https://doi.org/10.2118/187213-MS

Al-Murayri, M.T., Al-Kharji, A.A., Kamal, D.S., Al-Ajmi, M.F., Al-Ajmi, R.N., Al-Shammari, M.J., Al-Asfoor, T.H., Badham, S.J., Bouma, C., Brown, J., Suniga, H.P., 2018. Successful Implementation of a One-Spot ASP Pilot. Paper SPE-190374-MS. https://doi.org/10.2118/190374-MS

Al-Murayri, M.T., Sulaiman, D.S., Hassan, A.A., Al-Ajmi, N.A., Thery, B., Maillon, R., Nesbit, J., Pitts, M.J., Dean, E., Skeans, E., Dean, R.M., Britton, C.J., 2022. Encouraging Chemical EOR Field Results. Paper SPE-211449-MS. https://doi.org/10.2118/211449-MS

Carlisle, C., Al-Maraghi, E., Al-Saad, B., Britton, C., Fortenberry, R., Pope, G.A., 2014. One-Spot Pilot Results in the Sabriyah-Mauddud Carbonate Formation in Kuwait. Paper SPE-169153-MS. https://doi.org/10.2118/169153-MS

Flaaten, A.K., Nguyen, Q.P., Pope, G.A., Zhang, J., 2009. A Systematic Laboratory Approach to Low-Cost, High-Performance Chemical Flooding. SPE Res. Eval. Eng. 12, 713–723. https://doi.org/10.2118/113469-PA

Ghosh, P., Mohanty, K.K., 2019. Study of Surfactant-Polymer Flooding in High Temperature and High Salinity Carbonate Rocks. Energy Fuels 33, 4130–4145. https://doi.org/10.1021/acs.energyfuels.9b00407

Harden, C.J., 2014. Discount Rate Development in Oil and Gas Valuation. Paper SPE-169862-MS. https://doi.org/10.2118/169862-MS

Hazarika, K., Gogoi, S.B., Kumar, A., 2023. Polymer flooding and its effects on enhanced oil recovery special reference to Upper Assam Basin. Pet. Res. 8, 54–62. https://doi.org/10.1016/j.ptlrs.2022.03.003

Henthorne, L., Pope, G.A., Weerasooriya, U., Llano, V., 2014. Impact of Water Softening on Chemical Enhanced Oil Recovery Project Economics. Paper SPE-169165-MS. https://doi.org/10.2118/169165-MS

Hirasaki, G., Zhang, D.L., 2004. Surface Chemistry of Oil Recovery from Fractured, Oil-Wet, Carbonate Formations. SPE J. 9, 151–162. https://doi.org/10.2118/88365-PA

Humphry, K.J., Suijkerbuijk, B.M.J.M., van der Linde, H.A., Pieterse, S.G.J., Masalmeh, S.K., 2014. Impact of Wettability on Residual Oil Saturation and Capillary Desaturation Curves. Petrophysics 55, 313–318.

Jabbar, M.Y., Al Sowaidi, A., Al Obeidli, A., Willingham, T.W., Britton, C., Adkins, S., Delshad, M., Xiao, R., Teletzke, G.F., 2017. Chemical Formulation Design in High Salinity, High Temperature Carbonate Reservoir. Paper SPE-188604-MS. https://doi.org/10.2118/188604-MS

Karpan, V., Mahrooqi, D., Amri, N., Farsi, S., Dangi, S.L., Memon, A.R., Alimohammadiardakani, P., Pal, M., 2025. Advancing Surfactant-Based Chemical EOR in High-Salinity, High-Temperature Carbonate Reservoirs of Sultanate of Oman. Paper SPE-229924-MS. https://doi.org/10.2118/229924-MS

Lake, L.W., Johns, R.T., Rossen, W.R., Pope, G.A., 2014. Fundamentals of Enhanced Oil Recovery. Society of Petroleum Engineers.

Levitt, D.B., Jackson, A.C., Heinson, C., Britton, L.N., Malik, T., Dwarakanath, V., Pope, G.A., 2009. Identification and Evaluation of High-Performance EOR Surfactants. SPE Res. Eval. Eng. 12, 243–253. https://doi.org/10.2118/100089-PA

Levitt, D., Klimenko, A., Jouenne, S., Passade-Boupat, N., Cordelier, P., Morel, D., Bourrel, M., 2016. Designing and Injecting a Chemical Formulation for a Successful Offshore Chemical EOR Pilot. Paper SPE-179679-MS. https://doi.org/10.2118/179679-MS

Lim, S.S.S., Elochukwu, H., Nandong, J., Bennour, Z., Hamid, M.A., 2023. A review on the mechanisms of low salinity water/surfactant/nanoparticles and the potential synergistic application for c-EOR. Pet. Res. 8, 324–337. https://doi.org/10.1016/j.ptlrs.2023.02.001

Lu, J., Britton, C., Solairaj, S., Liyanage, P.J., Kim, D.H., Adkins, S., Arachchilage, G.W.P., Weerasooriya, U., Pope, G.A., 2014. Novel Large-Hydrophobe Alkoxy Carboxylate Surfactants for Enhanced Oil Recovery. SPE J. 19, 1024–1034. https://doi.org/10.2118/154261-PA

Masalmeh, S.K., 2013. Determination of Waterflooding Residual Oil Saturation for Mixed to Oil-Wet Carbonate Reservoir and Its Impact on EOR. Paper SPE-165981-MS. https://doi.org/10.2118/165981-MS

Maubert, M., Liyanage, P.J., Pope, G.A., Upamali, K.A.N., Chang, L., Ren, G., Mateen, K., Ma, K., Bourdarot, G., Morel, D., 2018. ASP Experiments in Indiana Limestone Using NaOH. Paper SPE-190187-MS. https://doi.org/10.2118/190187-MS

Mejía, M., Parra, J.E., Mejía, L., Pope, G.A., Balhoff, M.T., 2021. Experiments and Numerical Simulations of Chemical Enhanced Oil Recovery in Fractured Carbonate Rocks. J. Pet. Sci. Eng. 199, 108280. https://doi.org/10.1016/j.petrol.2020.108280

Mogensen, K., Masalmeh, S., 2020. A Review of EOR Techniques for Carbonate Reservoirs in Challenging Geological Settings. J. Pet. Sci. Eng. 195, 107889. https://doi.org/10.1016/j.petrol.2020.107889

Montes, J., Blin, N., Alvarez, A.E., Barrio, I., Panadero, A., Rodriguez, R., Coca, M., Trujillo, F., 2018. Novel Anionic Surfactant Formulation for High Temperature Carbonate Reservoirs. Paper SPE-190353-MS. https://doi.org/10.2118/190353-MS

Morel, D., Al-Amrie, O., Delattre, E., Cordelier, P., Greder, H., Rivero, M., Romero, C., Bursaux, R., Peltier, S., Levitt, D., 2016. Specific Procedure for an Offshore Chemical EOR One Spot Pilot. Paper SPE-181643-MS. https://doi.org/10.2118/181643-MS

Panthi, K., Mohanty, K.K., 2024. Development of Surfactant Formulation for High-Temperature Offshore Carbonate Reservoirs. Front. Chem. 12, 1408115. https://doi.org/10.3389/fchem.2024.1408115

ShamsiJazeyi, H., Verduzco, R., Hirasaki, G.J., 2014. Reducing Adsorption of Anionic Surfactant for Enhanced Oil Recovery: Part I. Colloids Surf., A 453, 162–167. https://doi.org/10.1016/j.colsurfa.2013.10.042

Sheng, J.J., 2011. Modern Chemical Enhanced Oil Recovery: Theory and Practice. Gulf Professional Publishing.

Sheng, J.J., 2014. A Comprehensive Review of Alkaline-Surfactant-Polymer (ASP) Flooding. Asia-Pac. J. Chem. Eng. 9, 471–489. https://doi.org/10.1002/apj.1824

Solairaj, S., Britton, C., Kim, D.H., Weerasooriya, U., Pope, G.A., 2012. Measurement and Analysis of Surfactant Retention. Paper SPE-154247-MS. https://doi.org/10.2118/154247-MS

Tackie-Otoo, B.N., Otchere, D.A., Abdul Latiff, A.H., Mohammed, M.A.A., Hassan, A.M., 2024. Evaluation of the Oil Recovery Potential and Cost Implication Analysis of Alternative ASP Formulations for Sandstone and Carbonate Reservoirs. ACS Omega 9, 20859–20875. https://doi.org/10.1021/acsomega.3c09590

U.S. Energy Information Administration (EIA), 2026. Short-Term Energy Outlook. Washington, DC: U.S. Energy Information Administration; Mar. 10, 2026. https://www.eia.gov/outlooks/steo/ [accessed 1 April 2026].

Upamali, K.A.N., Liyanage, P.J., Jang, S.H., Shook, E., Weerasooriya, U.P., Pope, G.A., 2018. New Surfactants and Co-Solvents Increase Oil Recovery and Reduce Cost. SPE J. 23, 2202–2217. https://doi.org/10.2118/179702-PA

Wang, Y., Al-Naabi, A.N., Al-Hasani, M.A., Al-Naabi, A.M., Al-Sinani, I.S., Al-Jabri, S.H., 2024. Surfactant Flood in a Tight Carbonate Reservoir in North Oman. Paper SPE-222062-MS. https://doi.org/10.2118/222062-MS

Weerasooriya, U.P., Pope, G.A., 2014. Alkoxy Carboxylate Surfactants. U.S. Patent 8,822,391.

World Bank, 2025. Commodity Markets Outlook, October 2025. World Bank Group. https://openknowledge.worldbank.org/handle/10986/42490 [accessed 1 April 2026].

Yonguep, E., Kapiamba, K.F., Kabamba, K.J., Chowdhury, M., 2022. Formation, stabilization and chemical demulsification of crude oil-in-water emulsions: A review. Pet. Res. 7, 459–472. https://doi.org/10.1016/j.ptlrs.2022.01.007

Zahedi, M., Saeedi Dehaghani, A.H., 2025. Mechanistic Evaluation of Surfactant Assisted Smart Water Flooding with Sulfate and Phosphate Anions. Sci. Rep. 15, 8764. https://doi.org/10.1038/s41598-025-17006-0

Zhou, N.C., Lu, M., Liu, F., Li, W., Li, J., Vaughan, S., Trine, E., Li, Z., Dean, M., Britton, C., 2021. Development of a Robust Low-Tension Surfactant Formula for Chemical Flooding. Paper SPE-207969-MS. https://doi.org/10.2118/207969-MS

Zhou, X., Al-Abdrabalnabi, R., Khan, S.Z., Kamal, M.S., 2021. Interrelationship of Capillary Number, Interfacial Tension, Injection Flow Rate and Temperature by Surfactant Flooding. Paper SPE-205749-MS. https://doi.org/10.2118/205749-MS